Ultrasound in Med. & Biol., Vol. 47, No. 6, pp. 1484–1494, 2021

0301-5629/$ - see front matter

https://doi.org/10.1016/j.ultrasmedbio.2021.02.014

● *Original Contribution*

SONOGRAPHIC 3-D POWER DOPPLER IMAGING ENHANCES RAPID ASSESSMENT OF MORPHOLOGIC AND PATHOLOGIC ARTERIOVENOUS FISTULA VARIATIONS

Franz Josef Putz,* Karin Pfister,† Tobias Bergler,* Miriam C. Banas,* Ernst Michael Jung,‡ Bernhard Banas,* and Wilma Schierling†

* Department of Nephrology, University Hospital Regensburg, Regensburg, Germany; † Department of Vascular Surgery, University Hospital Regensburg, Regensburg, Germany; and ‡ Department of Radiology, University Hospital Regensburg, Germany

(*Received* 25 *November* 2020; *revised* 13 *February* 2021; *in final from* 17 *February* 2021)

Abstract—Early detection of pathologic variations in an arteriovenous fistula (AVF) is essential for preventing fistula dysfunction in individuals undergoing hemodialysis. This study aimed to evaluate the clinical applicability of 3-D tomographic ultrasound (tUS) for rapid and simple visualization of AVF morphology and pathology. We assessed 53 AVFs in 50 consecutive patients using 3-D tUS including secondary, blinded reading. For all examinations, a high-end ultrasound (US) device was used with linear probe, attached to a tUS system to allow freehand 3-D scanning. Participants were examined by 2-D US and 3-D tUS with different raw data (B-mode, power Doppler, B-flow). Additional angiography was available for 15 participants with scheduled interventions. In all participants, 3-D tUS allowed a 3-D representation of AVFs in angiographic-like images with good image quality. The 2-D US assessment took 7.9 ± 4.0 min. A 3-D power Doppler scan required, on average, 1.4 ± 0.6 min. Diagnostic accuracy of blinded reading for pathologies was high (86.8% for aneurysms and 79.2% for stenoses). Bland–Altman plots showed an excellent correlation of 3-D tUS with 2-D US and angiography. 3-D tUS is an easily and rapidly applicable method for visualizing morphologic and pathologic AVF variations. Color-coded 3-D reconstruction of power Doppler data simplifies detection of perfused aneurysms and stenoses. (E-mail: franz-josef.putz@ukr.de)

Key Words: **Arteriovenous fistula, Ultrasound, 3-D imaging, Power Doppler, Hemodialysis.**

INTRODUCTION

Owing to the organ donor shortage, for most people with end-stage renal failure (approximately 86,000 in Germany in 2017) hemodialysis is the method of choice instead of renal transplantation (Gemeinsamer Bundesausschuss 2018). The quality of hemodialysis depends in particular on the length of hemodialysis sessions, dialyzer performance and the hemodialysis access.

Problems with the hemodialysis access enhance morbidity and hospitalization rates (Vascular Access 2006 Work Group 2006). Dialysis patients with catheters and arteriovenous grafts are especially at risk for complications, such as infections and access dysfunction. The US National Kidney Foundation has highlighted the importance of detecting early fistula dysfunction before thrombosis can develop and emergency intervention become needed (Vascular Access 2006 Work Group 2006). Early diagnosis of morphologic and pathologic alterations of an arteriovenous fistula (AVF) is essential to ensuring the long-term satisfactory use of a dialysis access.

Conventional 2-D US plays a key role in assessing AVFs and is well established for initially diagnosing access-related insufficiency of hemodialysis. For experienced sonographers, Doppler sonography provides an excellent tool for real-time imaging in routine assessment and in the initial evaluation of access-related failure in adults and children (Dumars et al. 2002; Doelman et al. 2005; Thalhammer et al. 2007; Visciano et al. 2014; Shroff et al. 2019; Nalesso et al. 2020).

High-quality AVF sonography calls for a great deal of practice in properly estimating hemodynamic changes. Pulsation, movement artifacts and angle dependence are unavoidable drawbacks of the Doppler methods (Schäberle et al. 2016). The correct grading of AVF

Address correspondence to: Franz Josef Putz, Department of Nephrology, University Hospital Regensburg, Franz-Josef-Strau-Allee 11, D-93953 Regensburg, Germany. E-mail: franz-josef.putz@ukr.de

stenosis is therefore difficult and often a reason for intensive discussions (Wo et al. 2017). In the future, modern US techniques such as vector flow imaging could add important information about the hemodynamics in AVFs (Brandt et al. 2016; Nguyen et al. 2020). 2-D US only allows visualization of one section of the AVF per image; it is not suited to producing a complete view of the entire fistula. Supplemental imaging techniques—angiography, contrast-enhanced computed tomography and magnetic resonance imaging—are therefore often used for additional diagnostic procedures in identifying possible causes of fistula dysfunction (Ko et al. 2005; MacDonald et al. 2018). With these tools, the entire AVF morphology can be visualized and pathologies illustrated in multiple views. However, they have possible side effects and are time consuming and unsuited for bedside application. Angiography requires puncturing the fistula or the afferent artery, making it invasive (Lamby et al. 2016, 2017). Individuals are exposed to nephrotoxic contrast agents and radiation, possibly causing impaired renal perfusion, reduced kidney function, hyperthyroidism and allergic reactions.

Therefore, an easily applicable, non-invasive and safe diagnostic tool is needed that will allow visualization of the entire course of an AVF to guide puncture techniques or perform additional diagnostic and therapeutic workups. In this pre-experimental study, we evaluate the clinical applicability of 3-D tomographic ultrasound (tUS) for visualizing the morphology and pathology of AVFs in routine assessments and in people with access-related failure.

MATERIALS AND METHODS

From January to March 2018, 50 consecutive patients with 53 arteriovenous fistulas were recruited from our dialysis unit. Eligible for the study were individuals with regular AVF function and those with acute AVF dysfunction. Excluded were individuals with pacemakers, owing to interference with the electromagnetic positioning system applied. An experienced sonographer performed all 2-D and 3-D ultrasound (US) examinations using a high-end US machine (Logiq E9, General Electric, Milwaukee, WI, USA) combined with a linear multi-frequency transducer (9L). In 15 cases, available angiographic examinations of the AVF were included in the analysis. Owing to ethics concerns, additional angiography was an option for participants who needed an interventional procedure, but not for purposes of the study alone.

The participants were examined in an upright or supine position. Use of 3-D tUS required adapting the amount of acoustic gel, to permit optimal ultrasonic coupling between the fistula and the transducer without compressing or distorting the fistula lumen. The fistula was first assessed with 2-D US B-mode and 2-D US color-coded Doppler sonography, followed by an evaluation of cross-sectional views of the entire AVF course from the anastomosis to the confluence into the deep vein. Whenever possible, power Doppler (PD) or B-flow scans were added. Hemodynamic assessment of the fistula was carried out according to the algorithm of Schäberle and Leyerer (2014) to identify dysfunctional grafts. Blood velocities and volume flow were determined in the longitudinal view after angle correction. The anastomosis width and flow velocity, as well as the volume flow of the fistula at the brachial artery, were measured as a mean of three readings of the arterial blood flow velocity and the corresponding blood vessel diameter. In the case of inadequate low blood volumes (<600 mL/min) or decreasing blood flow volumes, further measurements were added.

Before the 3-D tUS scan, the US machine was connected to the tUS system (tUS, PIUR Imaging, Munich, Germany). When attached to current US devices, this stand-alone device allows freehand 3-D scanning. The system takes 2-D US frames from the US machine's video output, matches each image with an electromagnetic positioning system and compiles a 3-D volume data set that can be analyzed cross-sectionally, comparable to computed tomography and magnetic resonance imaging. The image data were stored digitally in DICOM format (Digital Imaging and Communications in Medicine).

B-mode, PD and B-flow pre-sets were adjusted separately for each participant to obtain ideal settings for the 3-D images. For B-mode, gain and dynamic range were adapted to achieve a high contrast between the fistula lumen and the surrounding tissue, with the focus positioned on the deepest part of the fistula lumen. For PD and B-flow, gain was adjusted to achieve a completely filled vessel lumen without significant blooming artifacts or background flashes. After 3-D US acquisition, B-mode reconstructions required a manual cropping of the fistula borders. PD and B-flow reconstructions involved complete suppression of the gray-scale image of the primary US image and adaptation of the flow information for exclusive visualization of the color-coded PD or B-flow signal to visualize the borders of the AVF, so cropping was not necessary.

From three to five scans per fistula were performed. The best scans in B-mode and PD mode were selected for further analysis. In cases where the initial 2-D US evaluation with the B-flow technique was satisfactory, we added 3-D tUS together with the B-flow mode. 2-D evaluation and 3-D imaging were timed separately.

For each 3-D tUS scan, at least three measurements of the vessel diameter were taken at distinct anatomic landmarks (*e.g.,* the anastomosis region) and compared

with results from the 2-D US and angiography, if available. Differences between 2-D US, 3-D B-mode tUS, 3-D PD tUS and angiography were visualized in a Bland–Altman analysis (Bland and Altman, 1986).

Two readers independently analyzed the 3-D tUS images in a second reading. Reader 1 had all clinical and 2-D information, whereas reader 2 was unaware of the results of the 2-D US and all medical data. Both readers analyzed the 3-D tUS images for the presence of aneurysm and stenoses. Each reader graded image quality from 1 (excellent) to 6 (insufficient). Cross tables helped define the sensitivity, specificity, positive predictive value (PPV), negative predictive value (NPV) and diagnostic accuracy separately for each reader. Categorical data were analyzed with the χ^2 test. An inter-rater reliability analysis using Cohen's κ statistic was performed to determine consistency between the two independent readers; values $\geq$0.75 were regarded as showing good agreement, between 0.75 and 0.50 moderate agreement and <0.50 poor agreement. Differences were considered statistically significant at $p < 0.05$. Statistical analyses were conducted with SPSS version 24.0 (IBM Corporation, Armonk, NY, USA).

The study was cleared by the local ethics committee of the University of Regensburg (18-924-101). We obtained informed consent from our participants for all US examinations and data analysis.

RESULTS

Baseline characteristics and sonographic findings

A total of 53 AVFs were assessed with 2-D US and 3-D tUS in the Department of Nephrology, University Hospital Regensburg. The participants were 37 to 85 y old, with AVFs created an average of 73.4 ± 65.7 mo before the US assessment. We examined 48 participants with native AVFs (90.6%) and five (9.4%) with arteriovenous grafts. One arteriovenous graft was formed as a loop graft. Clinical signs of shunt dysfunction in the form of low blood flow or partial thrombosis were found in three participants. AVFs were predominantly on the left side (n = 42, 79.2%), and the sites were predominantly cubital (n = 21, 39.6%), followed by forearm (n = 18, 34.0%) and upper arm (n = 14, 26.4%).

AVFs showed a mean shunt blood flow volume of 1.53 ± 0.99 L/min. The mean blood flow velocity within the anastomosis was 222.6 ± 103.2 cm/s at a mean anastomosis width of 5.5 ± 2.9 mm. The 2-D US assessment took 7.9 ± 4.0 min. Participants characteristics and sonographic findings are shown in Table 1.

Table 1. Participant characteristics, sonographic findings and technical data

Participant characteristic	All participants (n = 53)
Age, y	63.8 ± 12.2
Sex (male/female), n (%)	36/17 (67.9/32.1)
Arteriovenous fistula, n (%)	48 (90.6)
Arteriovenous graft, n (%)	5 (9.4)
Side of fistula, n (%)	
Left	42 (79.2)
Right	11 (20.8)
Site of fistula, n (%)	
Forearm	18 (34.0)
Elbow	21 (39.6)
Upper arm	14 (26.4)
Age of the fistula, mo	73.4 ± 65.7
Sonographic finding	
Blood flow, L/min	1.53 ± 0.99
Peak velocity brachial artery, cm/s	186.6 ± 74.6
Diameter brachial artery, mm	6.3 ± 1.9
Anastomosis	
Width, mm	5.5 ± 2.9
Peak velocity, cm/s	222.6 ± 103.2
Presence of aneurysm, n (%)	36 (67.9)
Presence of stenosis, n (%)	24 (45.3)
Technical data	
Duration of 2-D ultrasound acquisition, min	7.9 ± 4.0
Duration of 3-D ultrasound acquisition, min	1.4 ± 0.6

3-D tomographic US

In all cases, sonographic scans could be recorded with the requisite quality for 3-D reconstruction. The average 3-D scan took 1.4 ± 0.6 min. The 3-D reconstructions in all 53 cases yielded good-quality images (mean grade, 2.23; reader 1: 1.96, reader 2: 2.49), with the entire fistula depicted in 100% of them. The afferent artery was visualized in 81.2% of cases, the anastomosis in 83.0% and the central venous junction in 7.6%. In our study, there was no difference in the rate of successful 3-D reconstructions of AVFs and arteriovenous grafts.

The amount of time spent on 3-D reconstructions, and their quality, depended on the raw material used (B-mode, PD, B-flow): With B-mode, the 3-D reconstruction took longer because the vessel lumen had to be selected in each slide of the 3-D block ("cropping"). The image quality of the 3-D B-mode reconstruction depended on the accuracy of cropping the vessel lumen (Fig. 1). Cropping of a B-mode scan took about 5–10 min on average, time that is not needed when using PD or B-flow scans as raw material for the 3-D scans. The 3-D B-mode tUS was not impaired by vibration artifacts (Fig. 1). PD and B-flow reconstructions required reduction of the grayscale image of the primary US image and adaptation of the flow information for exclusive visualization of the color-coded PD or B-flow signal. For these 3-D reconstructions, additional cropping of other slides from the scan proved unnecessary (Fig. 1). The reconstructions based on PD or B-flow showed a rising vulnerability to moving or vibrating artifacts, but they took less time than the B-mode reconstructions and correlated well with the morphology of the entire fistula. The highest rate of vibration artifacts

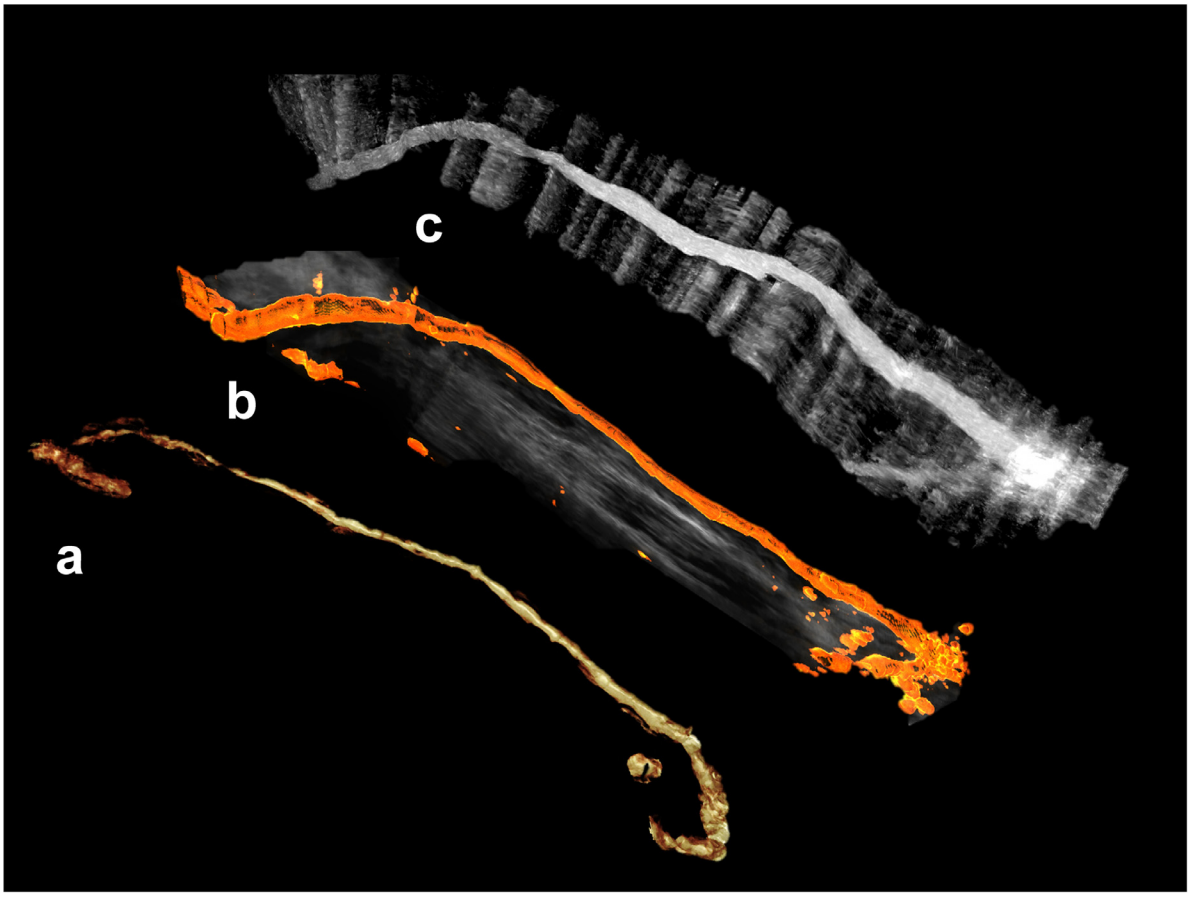

Fig. 1. Comparison of 3-D tomographic ultrasound (tUS) reconstructions of the same arteriovenous fistula (AVF) based on different raw data. (a) 3-D tUS cropped image of the AVF based on B-mode data. (b) 3-D tUS image of the AVF based on power Doppler data. (c) 3-D tUS image of the AVF based on B-flow data (digital flow technique).

was found in B-flow imaging, especially at the anastomosis site (Fig. 1).

In summary, the creation of 3-D images based on B-mode data was possible in all cases (53/53). The significantly faster reconstruction based on PD data was possible in 52/53 cases (98.1%). The only failed scan was owing to a thrombosed fistula with no blood flow. In contrast, reconstruction based on B-flow data was possible in only 20/53 cases (37.7%), mainly owing to high sensitivity to vibration artifacts. As a result of these vibration and motion artifacts, blood flow within the fistula could often not be clearly distinguished from the static environment.

Comparison of 3-D tUS with 2-D US and angiography

In this first preliminary study, 15 participants had a scheduled intra-vascular intervention, and thus complementary angiographies were available for direct comparison with 3-D tUS. Figure 2 shows a sample of images confirming the high technical quality of 3-D tUS, comparable with the current AVF diagnostic standard. They illustrate the congruence of 3-D PD tUS with the angiography of an AVF presenting a high-grade vein stenosis before and after balloon dilation. The reduced blood flow before balloon dilation caused a higher rate of artifacts; however, after restoration of the vessel diameter, 3-D PD tUS could record a precise image of the entire AVF that correlated well with the angiographic image. Aneurysm formation and tortuosity of the AVF were adequately captured by 3-D PD tUS and were congruent with the angiography (Fig. 3). 3-D PD tUS accurately showed local AVF vein stenosis that correlated with 2-D US (Fig. 4). Merging images of 3-D PD tUS with photographs of the participants enabled visualization of the entire course of the AVF and determination of suitable sites for cannulation (Figs. 3 and 4).

The 3-D B-mode tUS performed better than angiography and other sonographic flow techniques in visualizing low- or no-flow areas in or next to an AVF as hematoma, thrombosed pseudoaneurysm or abscess.

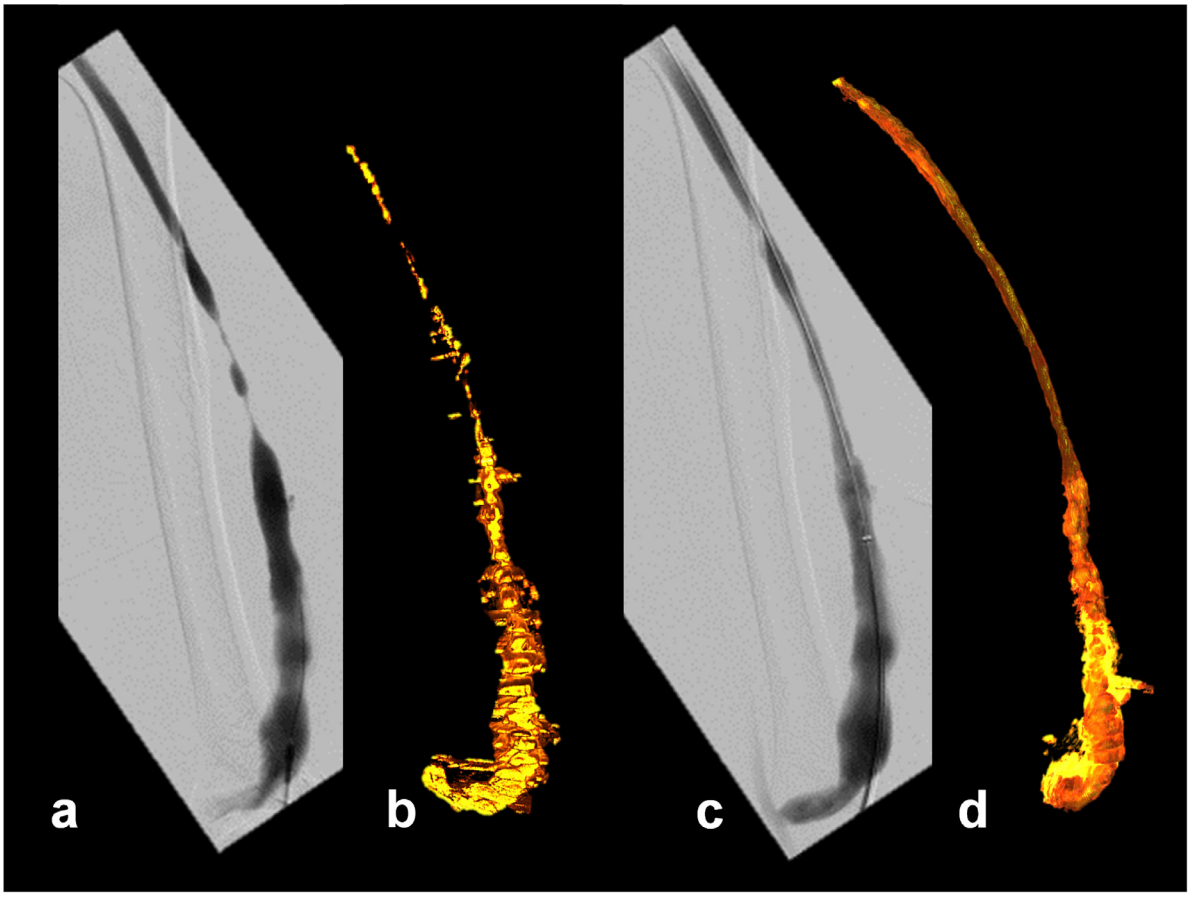

Fig. 2. 3-D tomographic ultrasound images and angiographies of an arteriovenous fistula (AVF) with a high-grade stenosis before and after balloon dilation. (a) Angiography of the AVF with a high-grade vein stenosis. (b) Corresponding 3-D tomographic ultrasound image on the basis of power Doppler of the AVF with the small diameter of the remaining lumen of the vein. (c) Angiography of the AVF after balloon dilation. (d) Corresponding 3-D tomographic ultrasound image of the AVF showing good agreement after successful dilation of the vein stenosis.

Examples include a non-perfused pseudoaneurysm (Fig. 5) and fluid accumulation around an AVF with clinical suspicion of infection (data not shown).

Besides the subjective ratings, Bland–Altman plots showed excellent agreement of 3-D tUS with 2-D US or angiography, with a difference of +0.012 mm between 2-D US and 3-D B-mode tUS and +0.091 mm between 2-D US and 3-D PD tUS (Fig. 6). In 15 cases, available angiographies served as benchmarks for the 3-D tUS measurements. Here, the difference between angiography and 3-D B-mode tUS amounted to +1.11 mm, and that between angiography and 3-D PD tUS to +1.20 mm (Fig. 6).

Reproducibility

Although there was no visual difference between the different 3-D tUS scans performed on the same participants in our study (three to five scans per fistula by an experienced sonographer), there are some technical issues that might limit the reproducibility of this technique between different examiners. Large aneurysmal AVFs with low blood flow volume were very susceptible to deformation owing to the contact pressure of the probe. Different contact pressures could therefore result in different cross-sectional diameters. Therefore, a lot of US gel was required to avoid changing the cross-sectional shape of the fistula. Straight-line lateral movements in the sense of rapid lateral displacement of the probe were technically difficult for the 3-D tUS software to compensate for and should be avoided during scanning. Patient movements relative to the magnetic field generator, as well as wide distances from the generator, could also lead to inaccurate measurements. Due to the limited applicability of 3-D tUS reconstructions based on B-flow data, repeatability of B-flow data might be difficult to accomplish, especially for untrained examiners.

Second reading

Using 2-D US and the clinical history, relevant aneurysms were identified in 67.9% of the AVFs (36/53)

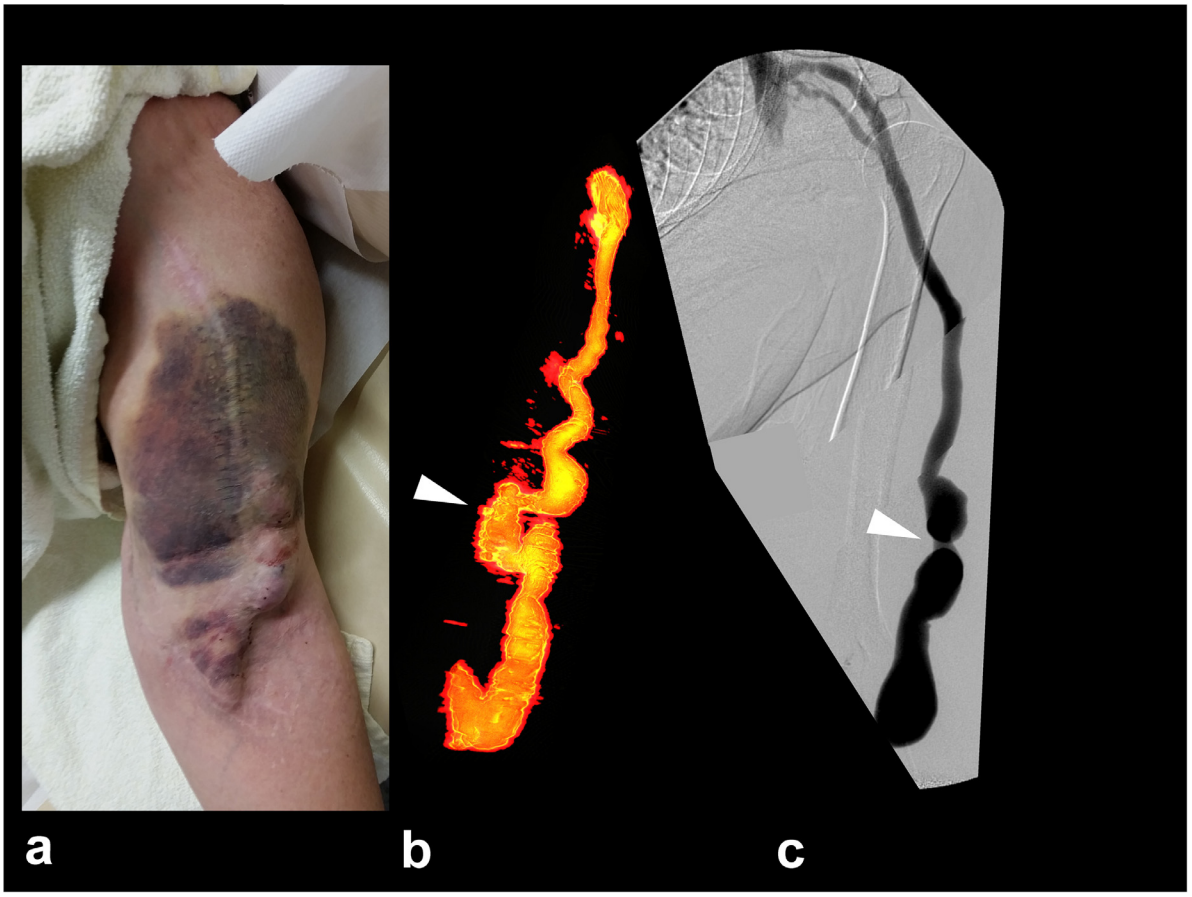

Fig. 3. Comparison of photography, 3-D ultrasound and angiography of an aneurysmatic arteriovenous fistula. (a) Photography of the participant's arm with post-dialytic hematoma after misplaced cannulation. (b) 3-D tomographic ultrasound reveals the kinking between both aneurysms causing the misplacement of dialysis cannula (*arrowhead*). (c) Angiography of the aneurysmatic arteriovenous fistula in posterior-anterior view. Kinking is hidden in this projection (*arrowhead*).

and relevant stenosis in 45.3% (24/53). Two independent readers performed a second reading of the 3-D tUS images for the presence of aneurysms and stenoses (one reader unblinded for the clinical issue and the volume flow of the AVF, and the other unaware of all additional information). For detecting aneurysms, the diagnostic accuracy of the unblinded reader was 100% (sensitivity, specificity, PPV and NPV all 100%; $\chi^2 = 53.000$: $p < 0.0001$: $\kappa = 1.000$). The blinded reader achieved a diagnostic accuracy of 86.8% (sensitivity, 80.6%; specificity, 100%; PPV, 100%; NPV, 70.8%; $\chi^2 = 30.242$; $p < 0.0001$; $\kappa = 0.727$). In detecting stenosis, the diagnostic accuracy of the unblinded reader was 98.1% (sensitivity, 95.8%; specificity, 100%; PPV, 100%; NPV, 96.7%; $\chi^2 = 49.099$; $p < 0.0001$; $\kappa = 0.962$), and that of the blinded reader was 79.2% (sensitivity, 66.7%; specificity, 89.7%; PPV, 84.2%; NPV, 76.5%; $\chi^2 = 18.114$; $p < 0.0001$; $\kappa = 0.574$). The diagnostic performance of both readers is shown in Table 2.

DISCUSSION

3-D US is an emerging field in modern US techniques, with applications in numerous areas of modern medicine. Cardiologists use it in diagnosing valvular defects, valve interventions and chamber quantifications (Utsunomiya et al. 2017; Lang et al. 2018). In obstetrics, the 3-D technique helps to diagnose pathologies of the child's face or fetal heart defects more easily (Tutschek et al. 2017; Chaoui et al. 2019).

In vascular surgery, 3-D tUS has already seen use in visualizing carotid stenosis and abdominal aortic aneurysms (Pfister et al. 2016; Pelz et al. 2017; Macharzina et al. 2020). The combination of contrast-enhanced US and 3-D tUS allows more sensitive detection than computed tomography of endoleaks in abdominal aortic aneurysms after endovascular therapy (Abbas et al. 2014).

Our investigation demonstrated the advantages of using 3-D tUS for routine assessment of AVFs and

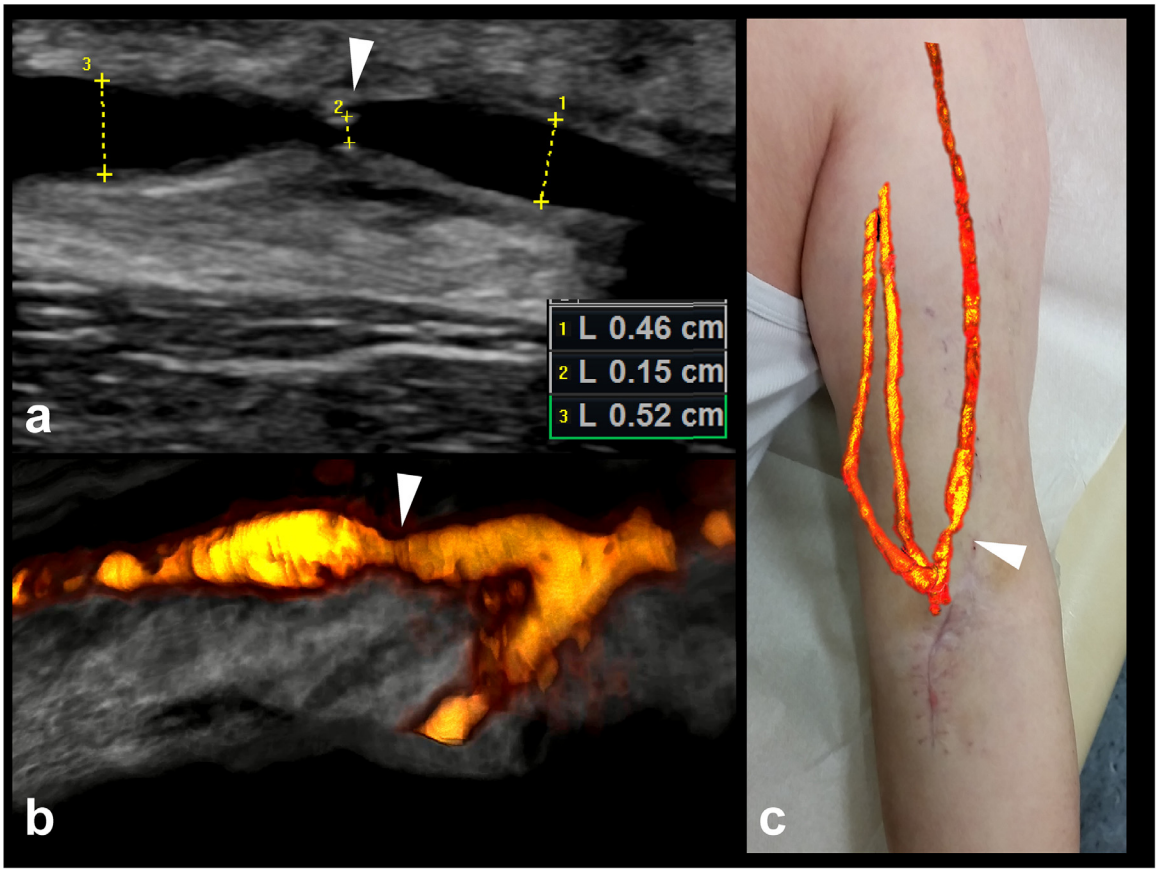

Fig. 4. Visualizing a high-grade stenosis in an arteriovenous fistula with 3-D tomographic ultrasound. (a) B-mode shows a high-grade stenosis of the vein of the arteriovenous fistula, with decreasing blood flow within the last 6 mo to 400 mL/min and evidence of dysfunction. (b) Visualization of the stenosis by 3-D ultrasound based on power Doppler. (c) The merged image of the 3-D ultrasound image and the participant's photography serves as a map for cannulation.

individuals with acute AVF dysfunction. These procedures currently rely primarily on 2-D US and Doppler techniques, which, however, demand a high-level skill set in duplex sonography (Schäberle and Leyerer 2014).

In line with earlier studies, we were able to obtain 3-D images by cropping the relevant structures within the 2-D raw data (Abbas et al. 2014). This not only is a time-consuming process but also requires a sonographer skilled in using the software.

In our approach, we suppressed the B-mode image information in the PD scan completely, so that only the borders of the AVF were visible. This makes the time-consuming cropping unnecessary and made a rapid overview of the AVF in an angiography-like picture possible, thus offering a tool for long-term surveillance and early detection of fistula-related problems. Because AVFs provided a continuous blood flow and pulsation artifacts were minimized, in almost all cases we were able to reconstruct 3-D images from blood flow visualized in the PD raw data. Color-coded Doppler sonography and determination of hemodynamic parameters can now be reserved for patients with specific, access-related dysfunction and angiography for those needing angioplasty or stent implantation.

Increasingly, specialists do the initial diagnosis of AVF dysfunction, while interventional radiologists or surgeons do the intervention or operation. 3-D tUS can provide objective image material that could transport the information from the first diagnostic assessment to the interventional radiologist or vascular surgeon. The entire visualization of the AVF permits estimation of the impacts of single stenoses on the function of the AVF, which is especially necessary in the case of multiple stenoses or the presence of "protective stenosis" in an AVF with a high blood flow volume.

The 3-D image allows the interdisciplinary team to discuss pathology and plan the entire procedure. In the future, the number of time-consuming and cost-intensive diagnostic angiographic procedures could be reduced by this easily applicable technique. Whether 3-D tUS can reduce the risk of hemodialysis needle displacement or improve the long-term surveillance of AVFs will require more studies.

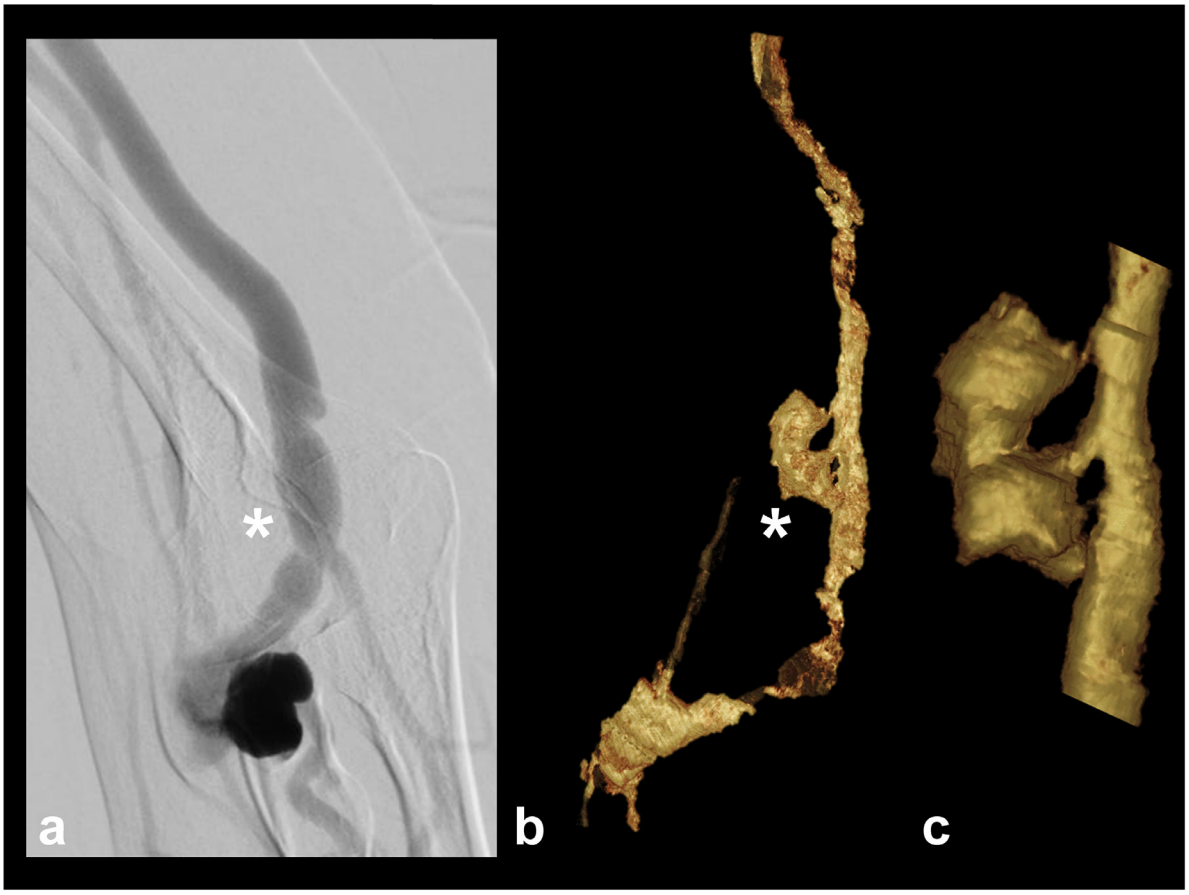

Fig. 5. Visualization of a non-perfused and clotted pseudoaneurysm next to an arteriovenous fistula (AVF) of a participant with repetitive cannulation problems. (a) Angiography of the AVF shows no evidence of the clotted pseudoaneurysm (*). (b) Corresponding 3-D cropped ultrasound image based on B-mode reveals the course of the AVF and the pseudoaneurysm (*) at former puncture sites. The pseudoaneurysm shows no evidence of blood flow and could consequently not be visualized by flow-based diagnostic procedures. (c) Magnification of the pseudoaneurysm with connection to the AVF (based on the initial 3-D ultrasound image).

Another advantage of 3-D tUS is that it does not expose the patient to radiation and nephrotoxic contrast agents. The optional use of an US contrast agent is dispensable because blood flow can be visualized non-invasively with power Doppler. Application of modern digital flow techniques (*e.g.,* B-flow; Weskott 2000; Jung et al. 2007) is another option; however, these methods are highly susceptible to tissue vibrations and thus artifact loading. Like angiographic techniques, methods based on blood flow are incapable of displaying no-flow areas (*e.g.,* hematomas, abscesses or pseudoaneurysms). In these cases, the B-mode raw data will have to be cropped for the 3-D images.

The costs of hospitalization for diagnostic angiographic procedures today still weigh on the delivery of care to hemodialysis patients (Vascular Access 2006 Work Group 2006). In contrast, AVF assessment using 3-D tUS can easily be performed bedside in dialysis centers, making it both cost-effective and time-saving.

Earlier publications reported that calcified plaques posed considerable difficulties in retrieving acceptable 3-D images of internal carotid artery stenosis. Calcified plaques with a consequent shadowing behind them also present a problem for sonographic 3-D imaging. For example, one study found that 3-D reconstruction of internal carotid artery stenosis was only possible in 84% of patients (Pelz et al. 2017). In our study, we showed in 100% of our cases that 3-D tUS reconstruction with satisfactory quality was possible, so relevant calcifications in the AVFs did not prevent adequate 3-D imaging.

This study has some limitations. As it is the first description of the use of 3-D tUS for visualization of AVFs, the results of this pre-experimental study need to be verified in further randomized trials with additional imaging modalities as controls. Due to the limited number of angiographies in this study, more cases with additional angiographies as controls should be considered in the future. Although there seems to be a good correlation

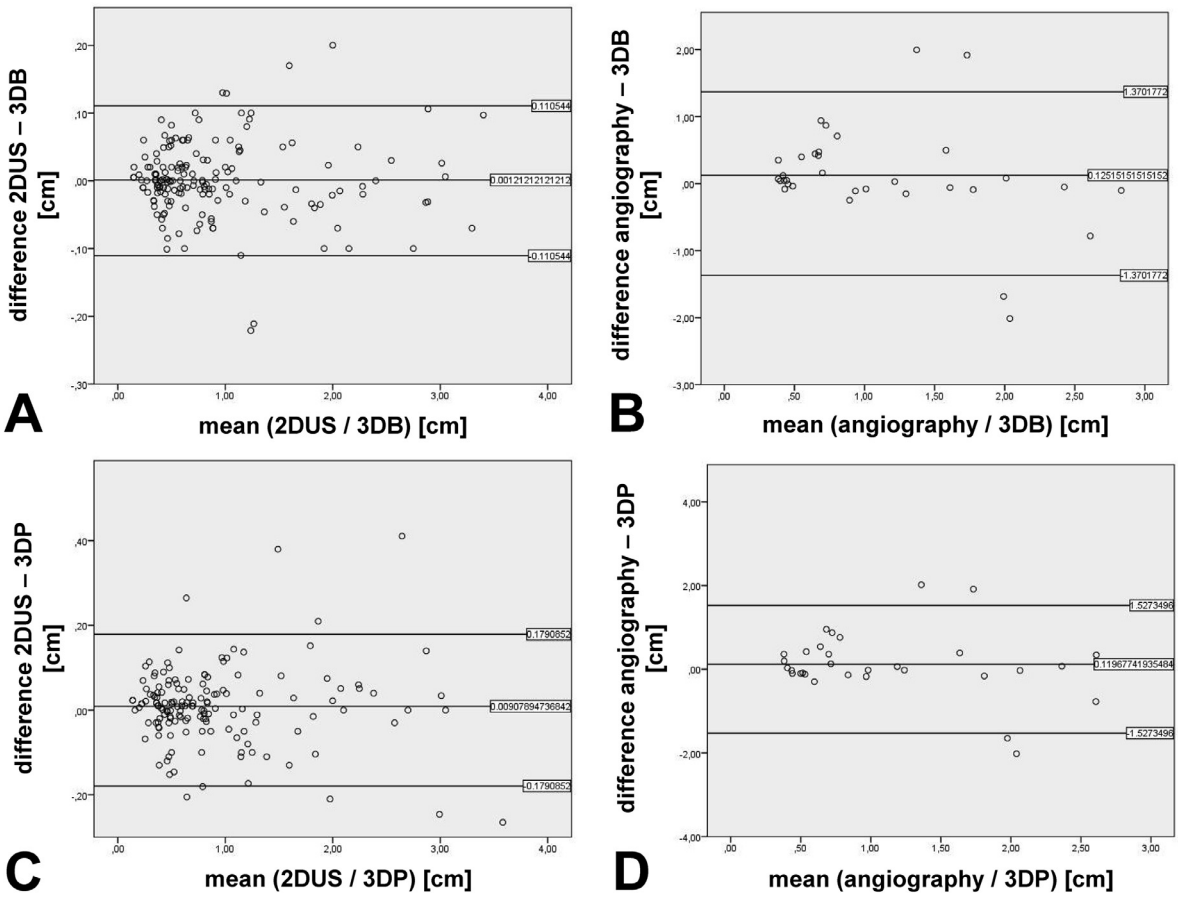

Fig. 6. Bland–Altman plots for agreement between methods used. Every 3-D tomographic ultrasound (tUS) scan was compared with at least three corresponding measurements of the vessel diameter at distinct anatomic landmarks (*e.g.,* the anastomosis region) to the results from the 2-D US or angiography. (a) Agreement between 3-D tUS based on B-mode (3-DB) and 2-D ultrasound for the measurement of different diameters within the arteriovenous fistula. The difference between 2-D US and 3-D B-mode tUS was +0.012 mm. (b) Agreement between 3-D tUS based on B-mode (3-DB) and angiography for the measurement of different diameters within the arteriovenous fistula. The difference between angiography and 3-D B-mode tUS was +0.091 mm. (c) Agreement between 3-D tUS based on power Doppler (3-DP) and 2-D ultrasound for the measurement of different diameters within the arteriovenous fistula. The difference between 2-D US and 3-D PD tUS was +1.11 mm. (d) Agreement between 3-D tUS based on power Doppler (3-DP) and angiography for the measurement of different diameters within the arteriovenous fistula. The difference between angiography and 3-D PD tUS was +1.20 mm.

of 3-D tUS with the current standard diagnostic 2-D US and angiography, and a good correlation between the two readers in the second reading, the inter-operator agreement needs to be verified in further studies.

Further possible technical limitations of 3-D tUS exist. Individuals with pacemakers or implantable cardioverter defibrillators must be excluded, because their devices could be disturbed by the external magnetic field; acquisition of fistula images of acceptable quality takes considerable practice; and detection of central venous stenosis by sonographic techniques is difficult, requiring additional diagnostic computed tomography

Table 2. Diagnostic accuracy of two independent readers

Condition	Reader	Sensitivity, %	Specificity, %	PPV, %	NPV, %	Diagnostic accuracy, %
Aneurysm	Unblinded reader	100	100	100	100	100
	Blinded reader	80.6	100	100	70.8	86.8
Stenosis	Unblinded reader	95.8	100	100	96.7	98.1
	Blinded reader	66.7	89.7	84.2	76.5	79.2

NPV = negative predictive value; PPV = Positive predictive value.

scans or angiography (Middleton et al. 1989; Finlay et al. 1993; Ko et al. 2005; Duijm et al. 2006).

CONCLUSIONS

In summary, 3-D tUS is a reliable screening tool that provides clear visualization of the morphology of AVFs, including existing pathologies, in an angiography-like image before an invasive angiography. Aneurysms and stenoses can be detected even by blinded readers. The technique is easy to use with some practice, and shows good correlation with 2-D US and angiography in this preliminary study. Moreover, it can be applied bedside without the use of harmful radiation or nephrotoxic contrast agents. Whether 3-D tUS can improve the surveillance and puncturability of AVFs in patient care needs to be investigated in further studies.

Acknowledgments—The authors thank "DHV-DE" for language editing. This work was supported by the University Hospital of Regensburg (ReForM B under a grant to F.J.P.). PIUR Imaging (Munich, Germany) provided the tomographic ultrasound system for 3 mo for data acquisition.

Conflict of interest disclosure—The authors declare no conflicts of interest. The results presented in this article have not been published previously in whole or part, except in abstract format.

REFERENCES

Abbas A, Hansrani V, Sedgwick N, Ghosh J, McCollum CN. 3 D contrast enhanced ultrasound for detecting endoleak following endovascular aneurysm repair (EVAR). Eur J Vasc Endovasc Surg 2014;47:487–492.

Bland JM, Altman DG. Statistical methods for assessing agreement between two methods of clinical measurement. Lancet 1986;1: 307–310.

Brandt AH, Jensen J, Hansen KL, Hansen P, Lange T, Rix M, Jensen JA, Lönn L, Nielsen MB. Surveillance for hemodialysis access stenosis: usefulness of ultrasound vector volume flow. J Vasc Access 2016;17:483–488.

Chaoui R, Abuhamad A, Martins J, Heling KS. Recent development in three and four dimension fetal echocardiography. Fetal Diagn Ther 2019;47:1–9.

Doelman C, Duijm LEM, Liem YS, Froger CL, Tielbeek AV, Donkers-van Rossum AB, Cuypers PWM, Douwes-Draaijer P, Buth J, van den Bosch HCM. Stenosis detection in failing hemodialysis access fistulas and grafts: comparison of color Doppler ultrasonography, contrast-enhanced magnetic resonance angiography, and digital subtraction angiography. J Vasc Surg 2005;42:739–746.

Duijm LEM, Liem YS, van der Rijt RHH, Nobrega FJ, van den Bosch HCM, Douwes-Draaijer P, Cuypers PWM, Tielbeek AV. Inflow stenoses in dysfunctional hemodialysis access fistulae and grafts. Am J Kidney Dis 2006;48:98–105.

Dumars MC, Thompson WE, Bluth EI, Lindberg JS, Yoselevitz M, Merritt CRB. Management of suspected hemodialysis graft dysfunction: usefulness of diagnostic US. Radiology 2002;222: 103–107.

Finlay DE, Longley DG, Foshager MC, Letourneau JG. Duplex and color Doppler sonography of hemodialysis arteriovenous fistulas and grafts. Radiographics 1993;13:983–989.

Jung EM, Kubale R, Clevert D-A, Weskott H-P, Prantl L, Herold T, Renz M, Rupp N, Tacke J. B-flow and B-flow with 3 D and SRI postprocessing before intervention and monitoring after stenting of the internal carotid artery. Clin Hemorheol Microcirc 2007;36: 35–46.

Ko SF, Huang CC, Ng SH, Lee TY, Hsieh MJ, Lee FY, Chen MC, Sheen-Chen SM, Lee CH. MDCT angiography for evaluation of the complete vascular tree of hemodialysis fistulas. AJR Am J Roentgenol 2005;185:1268–1274.

Lamby P, Jung F, Falter J, Mrowietz C, Graf S, Schellenberg L, Platz Batista da Silva N, Prantl L, Franke RP, Jung EM. Effect of radiographic contrast media on renal perfusion—first results. Clin Hemorheol Microcirc 2016;64:287–295.

Lamby P, Jung F, Graf S, Schellenberg L, Falter J, Platz-da-Silva N, Schreml S, Prantl L, Franke RP, Jung EM. Effect of iodinated contrast media on renal perfusion: A randomized comparison study in pigs using quantitative contrast-enhanced ultrasound (CEUS). Sci Rep 2017;7:13125.

Lang RM, Addetia K, Narang A, Mor-Avi V. 3-dimensional echocardiography: Latest developments and future directions. JACC Cardiovasc Imaging 2018;11:1854–1878.

MacDonald CJ, Gandy S, Avison ECM, Matthew S, Ross R, Houston JG. Non-contrast MRI methods as a tool for the pre-operative assessment and surveillance of the arterio-venous fistula for haemodialysis. MAGMA 2018;31:735–745.

Macharzina RR, Kocher S, Hoffmann F, Becher H, Kammerer T, Vogt M, Vach W, Fan N, Rastan A, Neumann F-J, Zeller T. Accuracy of carotid artery stenosis quantification with 4-D-supported 3-D power-Doppler versus color-Doppler and 2-D blood velocity-based duplex ultrasonography. Ultrasound Med Biol 2020;46:1082–1091.

Medical Netcare GmbH. Jahresbericht Datenanalyse Dialyse für den Gemeinsamen Bundesausschuss, Berichtsjahr 2017., https://www.g-ba.de/downloads/39-261-3410/2018-07-19_QSD-RL_MNC-Jahresbericht-2017.pdf. [accessed March 14, 2021].

Middleton WD, Picus DD, Marx MV, Melson GL. Color Doppler sonography of hemodialysis vascular access: comparison with angiography. AJR Am J Roentgenol 1989;152:633–639.

Nalesso F, Garzotto F, Muraro E, Cattarin L, Rigato M, Gobbi L, Innico G, Calò LA. Ultrasound for the clinical management of vascular access cannulation and needle position in hemodialysis patients. Ultrasound Med Biol 2020;46:455–459.

Nguyen TQ, Traberg MS, Olesen JB, Heerwagen ST, Brandt AH, Bechsgaard T, Pedersen BL, Moshavegh R, Lönn L, Jensen JA, Nielsen MB, Hansen KL. Flow complexity estimation in dysfunctional arteriovenous dialysis fistulas using vector flow imaging. Ultrasound Med Biol 2020;46:2493–2504.

Pelz JO, Weinreich A, Karlas T, Saur D. Evaluation of freehand B-mode and power-mode 3 D ultrasound for visualisation and grading of internal carotid artery stenosis. PLoS One 2017;12 e0167500.

Pfister K, Schierling W, Jung EM, Apfelbeck H, Hennersperger C, Kasprzak PM. Standardized 2 D ultrasound versus 3 D/4 D ultrasound and image fusion for measurement of aortic aneurysm diameter in follow-up after EVAR. Clin Hemorheol Microcirc 2016;62:249–260.

Schäberle W, Leyerer L. Strukturierte, zeiteffiziente und therapieorientierte Ultraschalldiagnostik bei Dialyseshuntproblemen. Gefasschirurgie 2014;19:471–480.

Schäberle W, Leyerer L, Schierling W, Pfister K. Ultrasound diagnostics of renal artery stenosis: Stenosis criteria, CEUS and recurrent in-stent stenosis. Gefasschirurgie 2016;21:4–13.

Shroff R, Calder F, Bakkaloğlu S, Nagler EV, Stuart S, Stronach L, Schmitt CP, Heckert KH, Bourquelot P, Wagner A-M, Paglialonga F, Mitra S, Stefanidis CJ. Vascular access in children requiring maintenance haemodialysis: a consensus document by the European Society for Paediatric Nephrology Dialysis Working Group. Nephrol Dial Transplant 2019;34:1746–1765.

Thalhammer C, Aschwanden M, Staub D, Dickenmann M, Jaeger KA. Duplex sonography of hemodialysis access. Ultraschall Med 2007;28:450–465 quiz 466–471.

Tutschek B, Blaas H-GK, Abramowicz J, Baba K, Deng J, Lee W, Merz E, Platt L, Pretorius D, Timor-Tritsch IE, Gindes L. Three-dimensional ultrasound imaging of the fetal skull and face. Ultrasound Obstet Gynecol 2017;50:7–16.

Utsunomiya H, Berdejo J, Kobayashi S, Mihara H, Itabashi Y, Shiota T. Evaluation of vegetation size and its relationship with septic pulmonary embolism in tricuspid valve infective endocarditis: A real time 3 DTEE study. Echocardiography 2017;34:549–556.

Vascular Access 2006 Work Group. Clinical practice guidelines for vascular access. Am J Kidney Dis 2006;48(Suppl. 1):S176–S247.

Visciano B, Riccio E, de Falco V, Musumeci A, Capuano I, Memoli A, Di Nuzzi A, Pisani A. Complications of native arteriovenous fistula: the role of color Doppler ultrasonography. Ther Apher Dial 2014;18:155–161.

Weskott HP. B-Flow—eine neue Methode zur Blutflussdetektion. Ultraschall Med 2000;21:59–65.

Wo K, Morrison BJ, Harada RN. Developing duplex ultrasound criteria for diagnosis of arteriovenous fistula stenosis. Ann Vasc Surg 2017;38:99–104.